



# FRET Visualization of Cyclic Stretch-Activated ERK *via* Calcium Channels Mechanosensation While Not Integrin $\beta 1$ in Airway Smooth Muscle Cells

Xin Fang, Kai Ni, Jia Guo, Yaqin Li, Ying Zhou, Hui Sheng, Bing Bu, Mingzhi Luo, Mingxing Ouyang\* and Linhong Deng\*

Institute of Biomedical Engineering and Health Sciences, School of Pharmacy & School of Medicine, Changzhou University, Changzhou, China

## OPEN ACCESS

### Edited by:

Jihye Seong,  
Korea Institute of Science and  
Technology, South Korea

### Reviewed by:

Tae-Jin Kim,  
Pusan National University, South  
Korea  
Dian Jing,  
Shanghai Jiao Tong University, China

### \*Correspondence:

Mingxing Ouyang  
mxouyang@cczu.edu.cn  
Linhong Deng  
dlh@cczu.edu.cn

### Specialty section:

This article was submitted to  
Signaling,  
a section of the journal  
Frontiers in Cell and Developmental  
Biology

Received: 03 January 2022

Accepted: 05 April 2022

Published: 19 May 2022

### Citation:

Fang X, Ni K, Guo J, Li Y, Zhou Y,  
Sheng H, Bu B, Luo M, Ouyang M and  
Deng L (2022) FRET Visualization of  
Cyclic Stretch-Activated ERK *via*  
Calcium Channels Mechanosensation  
While Not Integrin  $\beta 1$  in Airway Smooth  
Muscle Cells.  
Front. Cell Dev. Biol. 10:847852.  
doi: 10.3389/fcell.2022.847852

Mechanical stretch is one type of common physiological activities such as during heart beating, lung breathing, blood flow through the vessels, and physical exercise. The mechanical stimulations regulate cellular functions and maintain body homeostasis. It still remains to further characterize the mechanical-biomechanical coupling mechanism. Here we applied fluorescence resonance energy transfer (FRET) technology to visualize ERK activity in airway smooth muscle (ASM) cells under cyclic stretch stimulation in airway smooth muscle (ASM) cells, and studied the mechanosensing pathway. FRET measurements showed apparent ERK activation by mechanical stretch, which was abolished by ERK inhibitor PD98059 pretreatment. Inhibition of extracellular  $\text{Ca}^{2+}$  influx reduced ERK activation, and selective inhibition of inositol 1,4,5-trisphosphate receptor ( $\text{IP}_3\text{R}$ )  $\text{Ca}^{2+}$  channel or SERCA  $\text{Ca}^{2+}$  pump on endoplasmic reticulum (ER) blocked the activation. Chemical inhibition of the L-type or store-operated  $\text{Ca}^{2+}$  channels on plasma membrane, or inhibition of integrin  $\beta 1$  with siRNA had little effect on ERK activation. Disruption of actin cytoskeleton but not microtubule one inhibited the stretch-induced ERK activation. Furthermore, the ER  $\text{IP}_3\text{R}$ -dependent ERK activation was not dependent on phospholipase C- $\text{IP}_3$  signal, indicating possibly more mechanical mechanism for  $\text{IP}_3\text{R}$  activation. It is concluded from our study that the mechanical stretch activated intracellular ERK signal in ASM cells through membrane  $\text{Ca}^{2+}$  channels mechanosensation but not integrin  $\beta 1$ , which was mediated by actin cytoskeleton.

**Keywords:** cyclic stretch, mechanosensation, ERK, calcium channel, fluorescence resonance energy transfer

## INTRODUCTION

Mechanical forces associated with cyclic stretch play important roles in the control of vascular functions and pulmonary circulation homeostasis, and stretch exercise in ordinary life shows benefits in improving physical and mental health (Geneen et al., 2017; Fang et al., 2019). In medical emergency, however, mechanical ventilation with repetitive cyclic stretch can result in inflammation and lung tissue injury (Slutsky and Ranieri, 2014; Horie et al., 2016). In the past decades, mechanical stretch in regulating physiological functions and cellular signaling has attracted wide research

interests (Sadoshima and Izumo, 1993; Loperena et al., 2018; Chu et al., 2019; Ren et al., 2021). The mechanotransduction mechanism of mechanical stimulation to cellular biochemical signals has been a topic that is yet to be fully understood.

Physiologically, mechanical stimulations show fundamental roles in cell behaviors, tissue and organ developments, and disease-associated processes (Ingber, 2003; Mammoto et al., 2013; Qi et al., 2016). Several mechanisms have been discovered for the mechanical stimulations to biochemical signal transformations including cellular mechanosensitive components and extracellular matrix (Swaminathan and Glicerich, 2021). For instance, Polycystin-1, a large-size molecule with eleven transmembrane domains, has been shown to act as the mechanosensing component to modulate mechanical stretch-induced bone-cell differentiation (Dalagiorgou et al., 2013; Dalagiorgou et al., 2017). Membrane-localized ion channels TRPV4 and Piezo2 played central roles in calcium oscillation induced by physiological (8%) and injurious (18% of strain) levels of mechanical strains in chondrocytes, respectively (Du et al., 2020). Kim et al. investigated the mechanism of cellular  $\text{Ca}^{2+}$  signaling induced by pulling force using optical laser tweezers, and found that the endoplasmic reticulum (ER)  $\text{Ca}^{2+}$  release is mediated by both actin cytoskeleton and mechanosensitive  $\text{Ca}^{2+}$  channels on the plasma membrane (Kim et al., 2015).

Cellular biochemical activities are regulated by mechanical stretch at multiple levels. It has been observed for long that cells reorient themselves nearly perpendicular to the direction of cyclic stretch, and so does the actin cytoskeleton (Hayakawa et al., 2001; Wang et al., 2001; Jungbauer et al., 2008; Liu et al., 2008). Except for morphological changes, ATP release is visualized by induction of mechanical stretch in human airway smooth muscle (ASM) cells (Takahara et al., 2014), and the ATP release is regulated by  $\text{Ca}^{2+}$  signaling via caveolae-mechanosensitive pathway in alveolar epithelium (Diem et al., 2020). The level of total reactive oxygen species by mitochondrial and NADPH oxidases is increased under mechanical stretch in retinal pigment epithelial cells (Liang et al., 2019). Cyclic mechanical stretch also increases  $\beta_{\text{ID}}$ -integrin protein level and activates the downstream signaling proteins focal adhesion kinase (FAK) and RhoA (Zhang et al., 2007). The abundance of CD40 in endothelial cells is upregulated through transforming growth factor  $\beta 1$  signaling when co-cultured with smooth muscle cells under cyclic stretch stimulation (Korff et al., 2007). A recent study identified mechanical stretch-mediated transcriptome profile changes during skin regeneration including nine robust hub genes and six transcriptional factors-mRNA regulatory network (Liu W. et al., 2021). Cyclic stretch also regulates extracellular secretions of vascular smooth muscle cells including microvesicles and growth factors, leading to functional modulations of surrounding cells and tissues (Wang et al., 2017; Liu J.-T. et al., 2021).

Mechanical stretch has been shown to stimulate the MAPK family ERK1/2 and c-Jun NH2-terminal kinase (JNK), depending on the stress fiber strain but not FAK in endothelial cells (Correa-Meyer et al., 2002; Hsu et al., 2010; Schmidt et al., 2016). Alexander et al. reported stretch-induced ERK1/2 activation

mediated by phospholipase  $\text{A}_2$  (PLA $_2$ )-dependent release of arachidonic acid in renal epithelial cells (Alexander et al., 2004). Myosin II-regulated tension on the stress fibers shows positive correlation with ERK activation in fibroblasts (Hirata et al., 2015). Kim et al. reported that in mechanical stretch-induced loss of myelin proteins, the release of  $\text{Ca}^{2+}$  from endoplasmic reticulum (ER) resulted in ERK activation in oligodendrocytes (Kim et al., 2020). Although ERK activation by mechanical stretch has been well documented, it still remains to further characterize the mechanosensitive pathway for the mechanical-biomechanical coupling to activate ERK kinase.

Airway smooth muscle (ASM) cells, one major component of bronchial tissue underneath the epithelia, provide mechanical support and contraction force in the bronchial during breathing, and excessive ASM mass is related to airway hyper-responsiveness under asthmatic condition, which has been a treatment target (Zuyderduyn et al., 2008; Balestrini et al., 2021). As a chronic disease impacting a large population in the world, asthma can be characterized with airway inflammation, increased ASM mass and prolonged contraction in the bronchial (Zuyderduyn et al., 2008; Doeing and Solway, 2013). ERK also shows crucial roles in regulating ASM cell proliferation and interleukin expression in lymphocytes in asthma-related conditions (Burgess et al., 2008; Li et al., 2010). Here we applied fluorescence resonance energy transfer (FRET) biosensor to directly visualize cellular ERK activity induced by cyclic stretch in ASM cells which are under physiological stretch during breathing. The FRET biosensor allows to visualize the dynamic ERK activity in live cells along with subcellular resolution (Komatsu et al., 2011; Ponsioen et al., 2021), which provided the fine measurement of ERK activation during the cyclic stretch stimulation. Our work demonstrated in ASM cells that  $\text{Ca}^{2+}$  channels via actin cytoskeleton, particularly those channels on ER membrane, acted as the mechanosensing pathway to the downstream activation of ERK. Interestingly, the ER IP $_3$ R-dependent ERK activation by cyclic stretch was independent of upstream PLC-IP $_3$  signal, indicating possibly more mechanical mechanism for the IP $_3$ R activation.

## MATERIALS AND METHODS

### Chemical Reagents

2-Amino-ethoxydiphenyl borate (2-APB, 100  $\mu\text{M}$ ), Nifedipine (10  $\mu\text{M}$ ),  $\text{LaCl}_3$  (100  $\mu\text{M}$ ), Cytochalasin D (1  $\mu\text{M}$ ), Blebbistatin (20  $\mu\text{M}$ ), Nocodazole (1  $\mu\text{M}$ ), ML-7 (20  $\mu\text{M}$ ), the ROCK inhibitor Y27632 (20  $\mu\text{M}$ ), and phalloidin-TRITC were purchased from Sigma-Aldrich. Thapsigargin (TG, 10  $\mu\text{M}$ ) was purchased from Abcam, U73122 (10  $\mu\text{M}$ ) from MedChemExpress, and fibronectin from Corning. ITGB1 (Beta1) siRNA (Integrin siRNA, 30 nM) was purchased from Thermo Fisher Scientific.

### Cell Culture

Primary ASM cells were isolated from the tracheas of 6-8-week-old Sprague Dawley rats as described previously (approved by the Ethics Committee of Changzhou University on Studies Ethics, Grant No. NSFC 11532003) (Wang et al., 2016). The cells were maintained in low-glucose Dulbecco's modified Eagle's medium (DMEM, Sigma-Aldrich) supplemented with 10% fetal bovine

serum (FBS, Thermo), 100  $\mu\text{g}/\text{ml}$  penicillin, and 100 unit/ml streptomycin at 37°C with 5%  $\text{CO}_2$  in a humidified incubator.

## Construction of Nuclear Localized ERK FRET Biosensor (Nuc-ERK FRET)

To make nuclear localized ERK biosensor, the nuclear-exporting signal (NES) peptide in the construct was replaced with double nuclear-localized signal (NLS) peptide (2x Pro-Lys-Lys-Lys-Arg-Lys-Val). Briefly, ECFP DNA fragment with 2xNLS sequence at the C-terminal was amplified by PCR. Both the original construct and amplified ECFP fragment were digested by NotI and SalI restriction enzymes, followed by ligation of the two digested products together to generate Nuc-ERK FRET construct.

## Plasmid and siRNA Transfections

DNA plasmid and siRNA were transfected into ASM cells by using Lipofectamine3000 according to the manual protocol (Invitrogen). Briefly, cells were passaged in medium without antibiotics into 6-well plates the day before transfection. By following the protocol, 2.5  $\mu\text{g}$  biosensor DNA, 4  $\mu\text{l}$  P3000, and 4  $\mu\text{l}$  Lipofectamine3000 were mixed to assemble Lipid-DNA particles for each well before adding it into the cell culture. The medium was changed in 8 h and cell imaging experiments were performed 40–64 h later.

For siRNA co-transfection, when cells reached 60%–80% confluency, siRNA (30 nM) was transfected into the cells with 4  $\mu\text{l}$  Lipofectamine3000 reagent. The medium was changed in 8 h, and after siRNA transfection for 24 h, the ERK FRET biosensor DNA was further transfected into the cells.

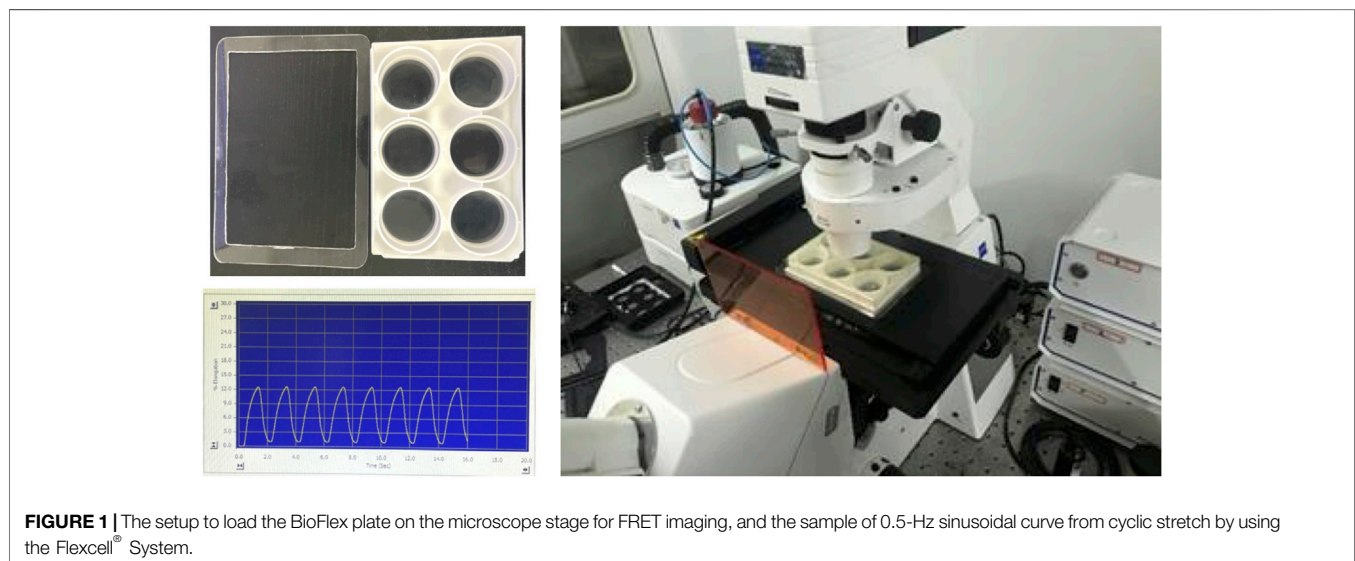
## Verification of ITGB1 siRNA Transfection Efficiency by qPCR

The efficiency of ITGB1 siRNA transfection was assessed with mRNA expression using Real-Time Quantitative PCR (qPCR)

assay. Total RNA from cultured ASM cells was extracted using the TRI Reagent RNA Isolation Reagent (#T9424, Sigma). Total RNA weighing 500 ng was applied to generate 1st strand cDNA by using the Revert Aid First Strand cDNA Synthesis Kit (#K1622, Thermo, MA). The sequences of associated qPCR primers for rat ITGB1 were derived from the previous report including GAATGGAGTGAATGGGACAGGAG (ITGB1 forward), CAGATGAACTGAAGGACCACCTC (ITGB1 reverse), and the control GAPDH primers AGGTCGGTGTGAACGGATTG (forward) and GGGGTCGTTGATGGCAACA (reverse) (Luo et al., 2018). The primers were synthesized from General Biosystems (Anhui, China), and PowerUp SYBR Green Master Mix (#A25742, Applied Biosystems, CA) was used for PCR amplification. The reaction was run in the qRT-PCR system (StepOnePlus, Applied Biosystems) with 1  $\mu\text{l}$  of the cDNA in a 10  $\mu\text{l}$  reaction according to the manufacturer's instructions. Calibration and normalization were done using the  $2^{-\Delta\Delta\text{CT}}$  method, where  $\Delta\Delta\text{CT} = \text{CT}(\text{target gene}) - \text{CT}(\text{reference gene})$ , and CT referred to the PCR cycle number by reaching the defined fluorescence intensity. Fold changes in mRNA expression were calculated based on the resulting CT values from three independent experiments.

## Mechanical Stretch

After DNA transfection for 24 h, cells were detached using Accutase solution (Sigma), and transferred to collagen I and fibronectin (40  $\mu\text{g}/\text{ml}$ ) double-coated 6-well BioFlex plates (Flexcell International Corporation, Hillsborough, NC, United States). After which the cells were cultured in the medium containing 1% FBS for 12–16 h and reached 60–80% confluence before the mechanical stretch. Cyclic stretch was applied with a 0.5-Hz sinusoidal curve at 12% elongation by using a Flexcell<sup>®</sup> FX-5000<sup>™</sup> Tension System (Flexcell<sup>®</sup> International Corporation). The computer program-controlled bioreactor used vacuum and positive air pressure to apply cyclic strain to cells cultured on flexible-bottomed BioFlex plates. After



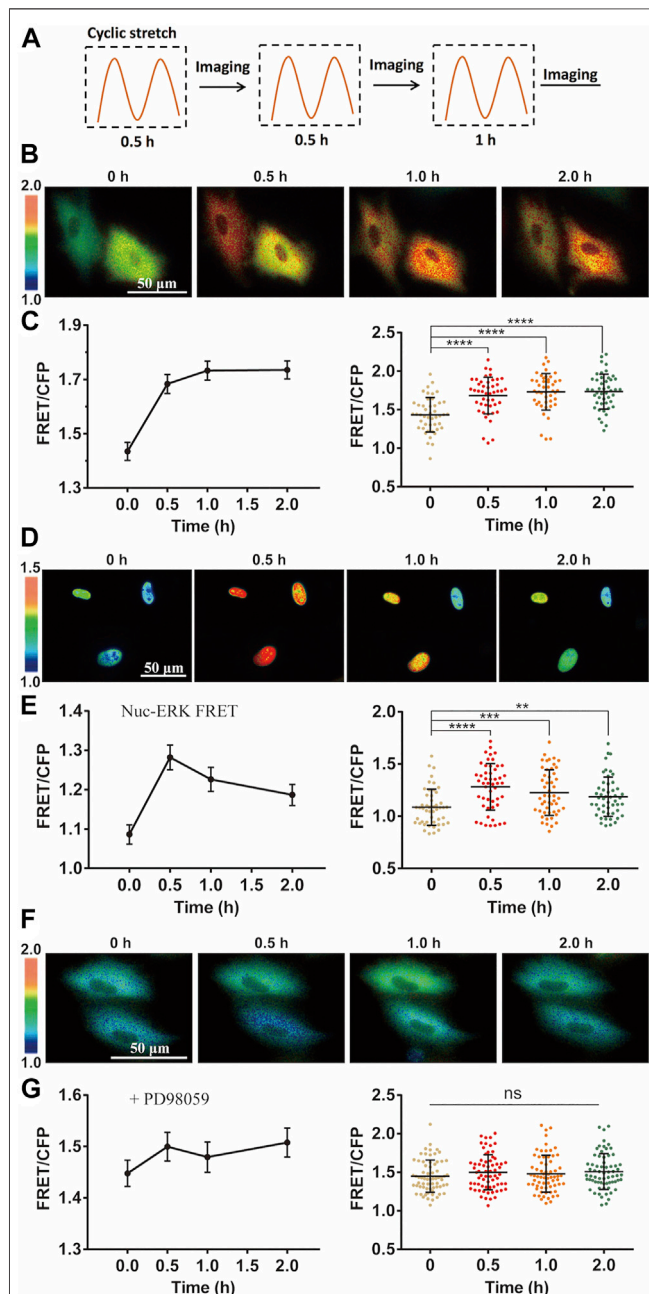


**FIGURE 2** | Cyclic stretch-induced ERK activation by FRET measurements. FRET/ECFP emission ratiometric images show the activation of ERK by cyclic stretch in ASM cells pre-incubated in 1% FBS culture medium. Scale bar = 50  $\mu$ m. **(A)** Illustrated experimental procedures of cyclic stretch stimulation (with a 0.5-Hz sinusoidal curve at 12% elongation deformation) followed by FRET imaging in multiple cycles. **(B,C)** ERK FRET ratio (YPet/ECFP) images **(B)**, and quantifications of the FRET changes in curves (Mean  $\pm$  S.E.M.) and scattering dots (Mean  $\pm$  S.D.  $n = 46$ ) **(C)** after cells were stimulated with cyclic stretch for the indicated time. **(D,E)** FRET images with Nuc-ERK FRET biosensor in cells **(D)**, and their statistical quantifications ( $n = 50$ ) **(E)** after cyclic stretch at the indicated time points. **(F,G)** ERK FRET images **(F)** and FRET statistical quantifications ( $n = 67$ ) **(G)** in cells pre-treated with 10  $\mu$ M PD98059 inhibitor for 1 h. Student's t-test was performed between the control and one experimental group, and multiple rounds of t-test  
(Continued)

**FIGURE 2** | were done for the variable experimental conditions. \*, \*\*, \*\*\*, and \*\*\*\* indicate  $p < 0.05$ , 0.01, 0.001, and 0.0001 from Student's t-test analysis while 'ns' for no significant difference, and so on through the paper.

the durations of cyclic stretch, the BioFlex plates with cells were moved from the Flexcell incubator to Zeiss microscopy for FRET imaging. The images of a group of cells were acquired within 10 min for each well.

## FRET Microscopy Imaging

The processes of FRET imaging and quantification were similar to our recent descriptions (Ouyang et al., 2019; Yao et al., 2020). Briefly, the Zeiss microscopy system (Zeiss Cell Observer) was equipped with the functions of multi-positions, fine auto-focusing, and automatic-switchable dichroic rotator. The scope stage was supplemented with an incubator box (Zeiss) to maintain temperature at 37°C and 5% CO<sub>2</sub> for live cell samples. During FRET image acquisitions through ECFP and FRET (YPet) channels, the parameters for excitation filter and dichroic mirror were  $436 \pm 10$  and 455 nm, respectively, and the emission filters of ECFP and FRET (YPet) channels were  $480 \pm 20$  nm and  $535 \pm 15$  nm, respectively.

To take the FRET images before and after the cyclic stretch, we made an accessory holder with acrylic plate to load the BioFlex plate on the microscopy stage, as shown in **Figure 1**. Before starting the stretch, 15–20 positions of fluorescent cells were selected per well, and FRET images were acquired as the pre-stretch condition. After the duration (0.5–1 h) of cyclic stretch, the same positions of cells were reloaded with minor adjustments, and the FRET images were taken within 10 min for each well before the next cycle.

## FRET Quantification and Statistical Analysis

FRET quantifications were processed using the Wang Lab (UCSD)-developed software package FluoCell in MATLAB (available on <http://github.com/lu6007/fluocell>) (Qin et al., 2019). Fluorescence signals from ECFP and FRET (YPet) images were measured after background subtractions, and the ratio of the two channels was calibrated in the pixel-to-pixel manner. Data procession and statistical analysis were done by the software of Graphpad Prism 6, and Excel. The quantified FRET data from a group of cells was expressed in curves (Mean  $\pm$  S.E.M.), and scattering dots (Mean  $\pm$  S.D.). \*, \*\*, \*\*\* and \*\*\*\* indicate  $p < 0.05$ , 0.01, 0.001, and 0.0001 from Student's t-test, which was applied for significant difference analysis. Multiple times of t-test analysis done between the control and one experimental group were carried for variable experimental conditions using Graphpad Prism 6. All described FRET experiments have been repeated independently on different days with similar conclusions, and statistical quantifications were performed based on the data acquired from different time.

## RESULTS

### Cyclic Mechanical Stretch-Induced ERK Activation Measured by FRET Biosensor

To understand how mechanical stimulation from cyclic stretch activates biochemical signals in live cells, we applied FRET

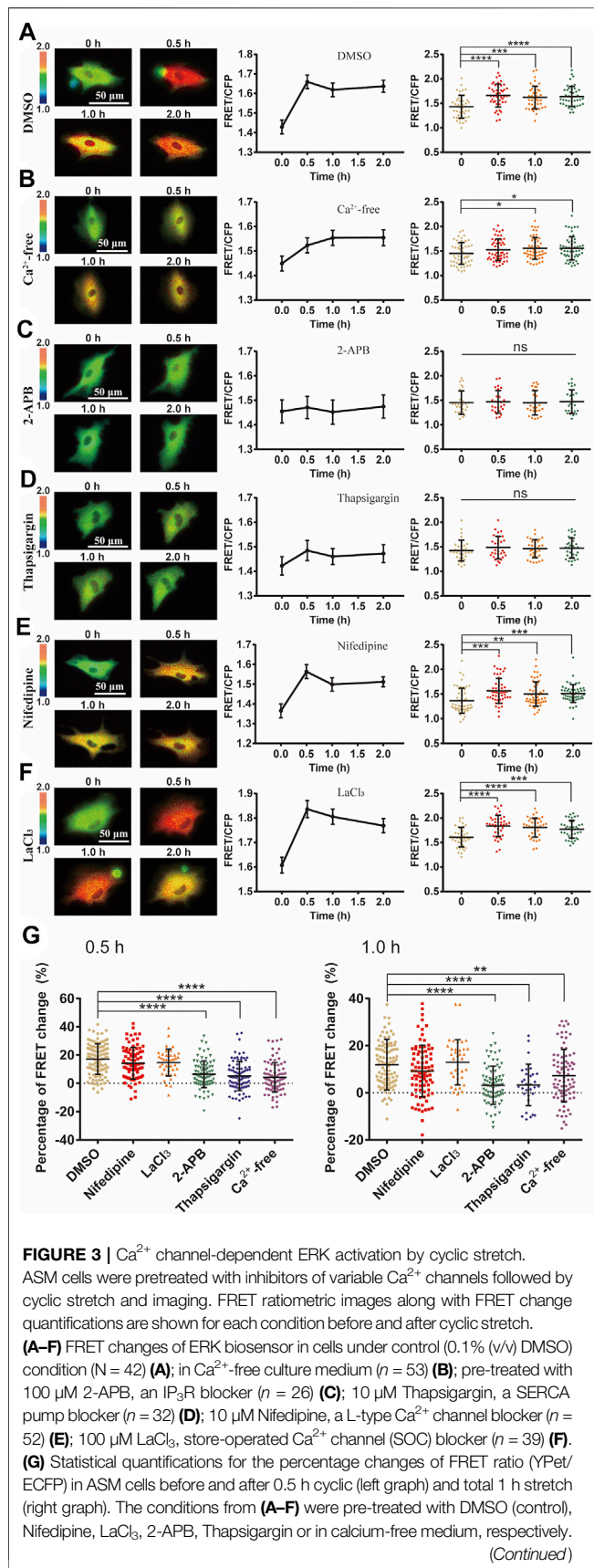


**FIGURE 3 |** n = 108, 87, 39, 84, 90/32, 83 in the indicated order. Student's t-test was performed between the control and one experimental group, and multiple rounds of t-test were done for the variable experimental conditions.

biosensor to measure ERK kinase activity in ASM cells. According to the previous study (Takahara et al., 2014), 12% strain deformation with a 0.5-Hz sinusoidal curve was within the physiological scale and was applied on the cells seeding on the elastic membrane by the Flexcell<sup>®</sup> Tension System, which could induce alignment of cells perpendicularly to the stretch direction in 7.5 h (Supplementary Figure S1). In regarding the inapplicability of visualizing the FRET signals on the microscope simultaneously during the cyclic stretch, the procedures were carried out in the following process: the FRET images were taken after 0.5 h-stretch followed by another 0.5 h-stretch and imaging, and then continued with one more 1 h-stretch and imaging (depicted in Figure 2A). The imaging was usually done within 10–30 min between the three times of stretch, and images of similar cell positions were acquired each time.

Intracellular ERK in the cytoplasm was activated by the mechanical stretch, as seen by the FRET changes (Figure 2B). FRET quantification from a group of cells showed apparent activity increase with statistical significance (Figure 2C). As control, no apparent FRET change was observed in the similar imaging procedure without stretch stimulation (Supplementary Figure S2). The platelet-derived growth factor (PDGF) regulates ERK activity in ASM cell proliferation and also inflammation in asthmatic condition (Lee et al., 2001; Kardas et al., 2020). The magnitude of ERK FRET change (~15–20%) from the mechanical stretch was comparable to PDGF-stimulated FRET change in ASM cells (Supplementary Figure S3). In consideration of ERK shuttling between the cell cytoplasm and nucleus, we modified the ERK biosensor to generate nuclear localized version Nuc-ERK FRET. As shown in Figures 2D,E, nuclear ERK was also activated by the mechanical stretch, which indicates the cytoplasmic increase is not due to nuclear ERK transportation. Hence, we used cytoplasmic FRET measurement to represent the whole cells in the following study. The ERK activation reported by FRET signals was verified by increased phosphorylation level of ERK with phospho-ERK antibody immunoblotting under the cyclic stretch (Supplementary Figure S4). The 12% strain deformation of ASM cells is within the physiological range of stretch magnitude (Takahara et al., 2014), which is also seen by the maintained cell shape (Figure 2B) and actin stress fibers (Supplementary Figure S5) after stretch. We further pretreated the cells with ERK inhibitor PD98059, which abolished stretch-induced FRET signals (Figures 2F,G), hence the FRET changes truly reported ERK activity.

## $\text{Ca}^{2+}$ Channel-Dependent ERK Activation by Cyclic Stretch

We then investigated the mechanosensitive components in transducing the mechanical stimulation into biochemical signals in cells.  $\text{Ca}^{2+}$  channels located on plasma membrane or endoplasmic reticulum (ER) are sensitive to

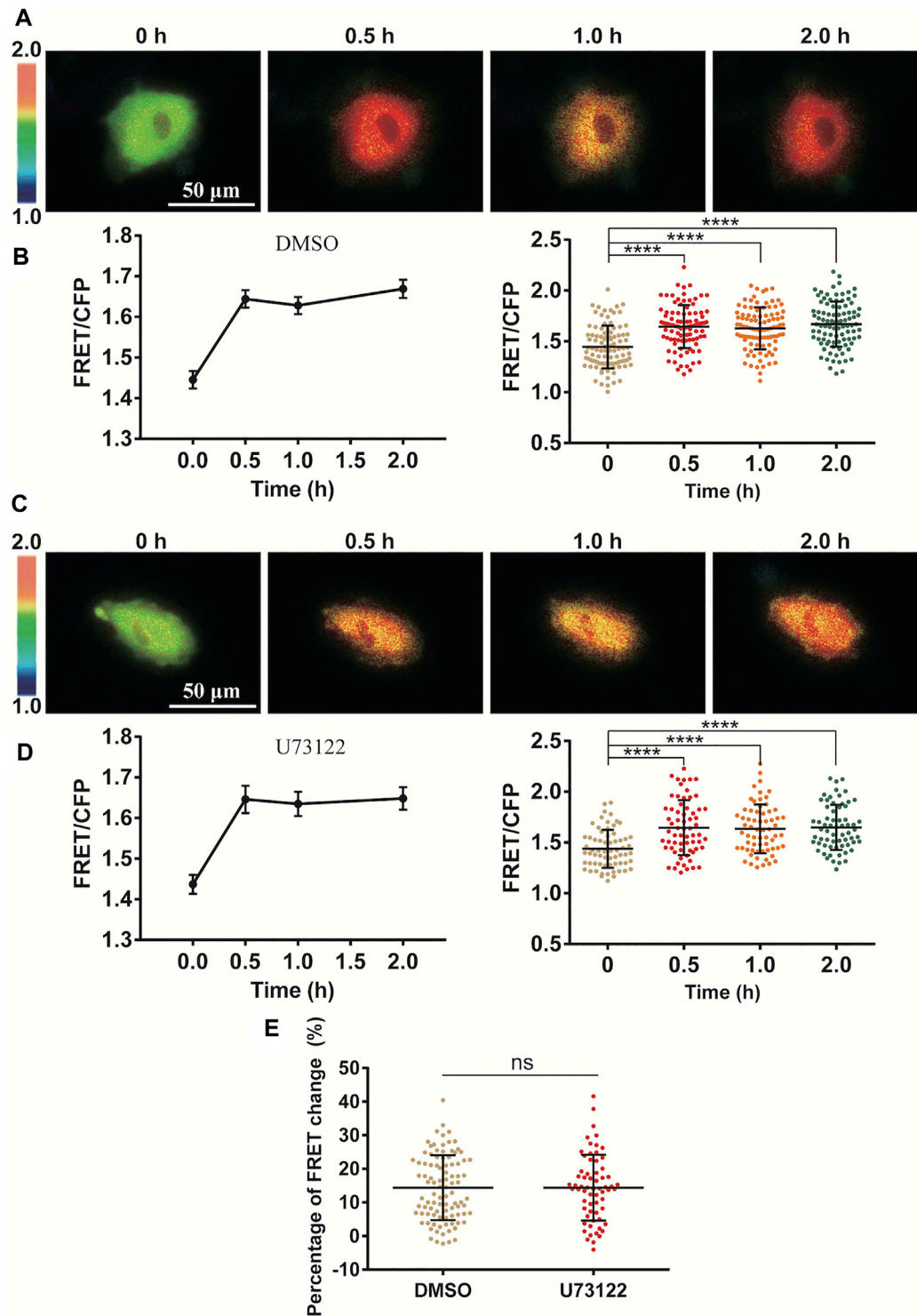


**FIGURE 4** | Independence of PLC-IP<sub>3</sub> signal for cyclic stretch-induced ERK activation. ASM cells were pretreated with PLC inhibitor U73122 (10  $\mu$ M) for 1.5 h followed by cyclic stretch. **(A–D)** FRET ratiometric images and quantification of FRET changes before and after cyclic stretch under the conditions of control (DMSO) **(A,B)** and U73122 treatment **(C,D)**. **(E)** Statistical comparison of FRET changes between the control ( $n = 96$ ) and U73122 ( $n = 65$ ) treatment after 0.5 h cyclic stretch, which is based on FRET data from three independent experiments. Student's t-test was performed between the control and one experimental group.

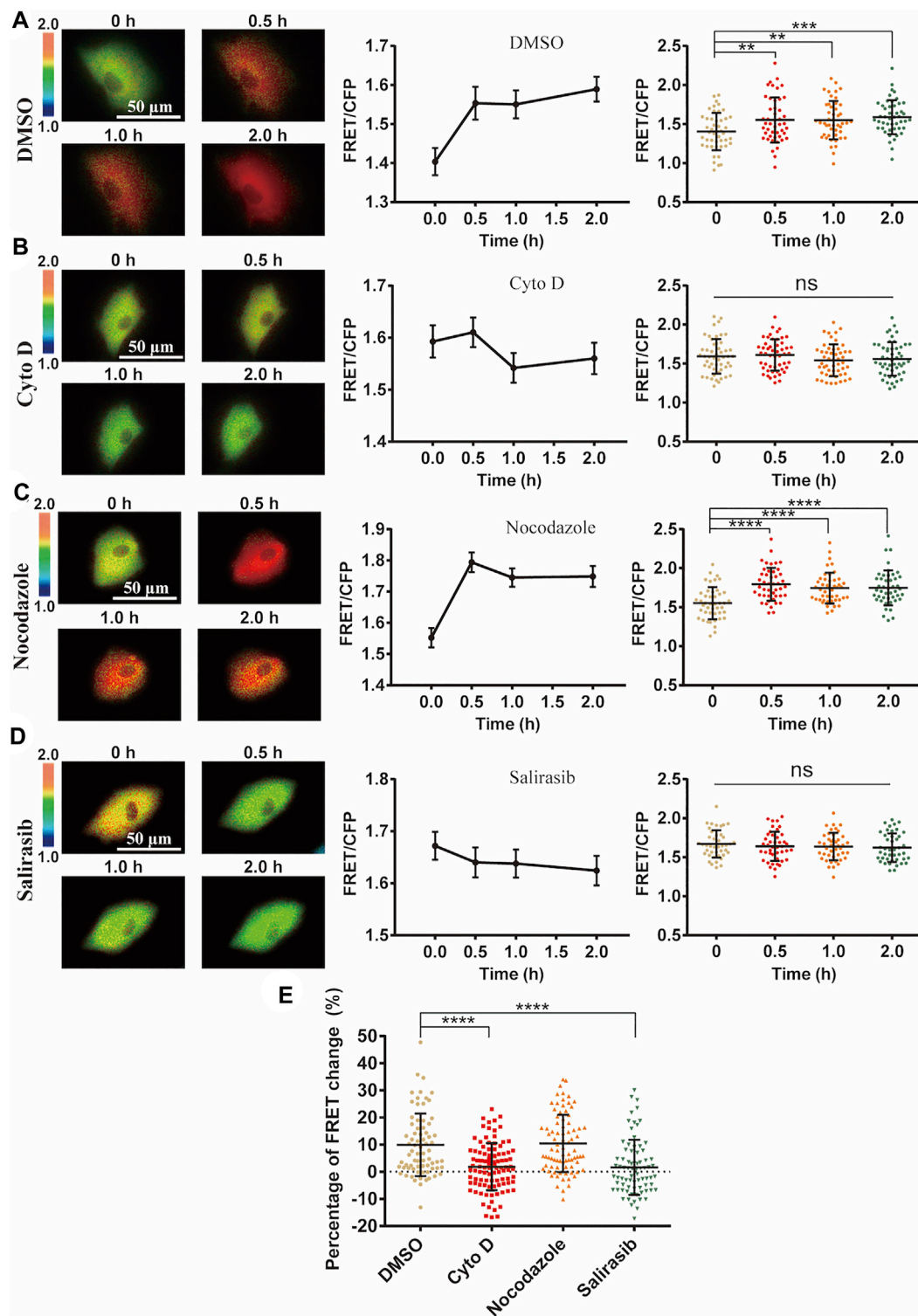


**FIGURE 5 |** Role of cell cytoskeleton on cyclic stretch-induced ERK activation. ASM cells were pretreated with cytoskeleton or Ras inhibitors, followed by cyclic stretch and imaging. FRET ratiometric images along with change quantifications are shown for each condition before and after cyclic stretch. **(A–D)** ERK FRET ratiometric images and statistical quantifications of FRET changes in ASM cells pretreated with DMSO ( $n = 47$ ) **(A)**, 1  $\mu$ M Cyto D ( $N = 51$ ) **(B)**, 1  $\mu$ M Nocodazole ( $n = 45$ ) **(C)**, and 75  $\mu$ M Ras inhibitor Salirasib ( $n = 43$ ) **(D)**. **(E)** Statistical comparisons of FRET percentage changes in ASM cells pre-treated with DMSO, Cyto D, Nocodazole, and Salirasib ( $n = 73, 99, 82, 77$ ) **(A–D)** before and after 0.5 h cyclic stretch, based on image data from two independent experiments. Student's t-test was performed between the control and one experimental group.

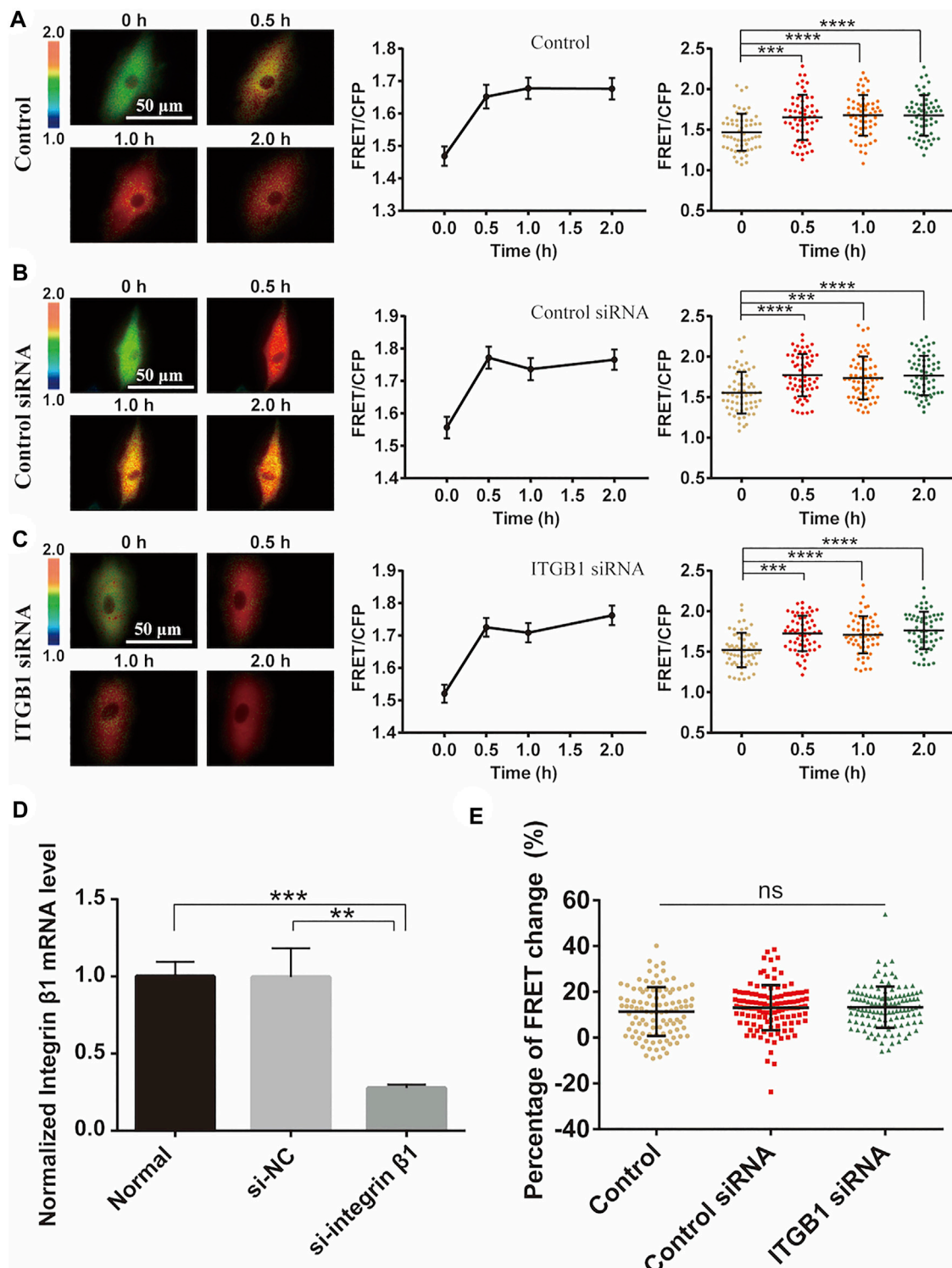


**FIGURE 6 |** Integrin  $\beta 1$  (ITGB1) signal in cyclic stretch-induced ERK activation. ASM cells were transfected with ITGB1 inhibitory siRNA, followed by cyclic stretch and imaging. **(A–C)** FRET ratiometric images along with FRET change quantifications are shown before and after cyclic stretch in ASM cells without transfection **(A)**, or transfected with control scramble siRNA **(B)** and ITGB1 siRNA **(C)** ( $n = 58, 60, 58$ ), respectively. **(D)** qPCR quantification from three experimental data confirmed the reduced level of ITGB1 mRNA expression after siRNA transfection. **(E)** Statistical comparisons of FRET percentage changes in cells without transfection, or transfected with control or ITGB1 siRNA ( $n = 103, 116, 121$ ) **(E)** before and after 0.5 h stretch. Student's t-test was performed between the control and one experimental group.

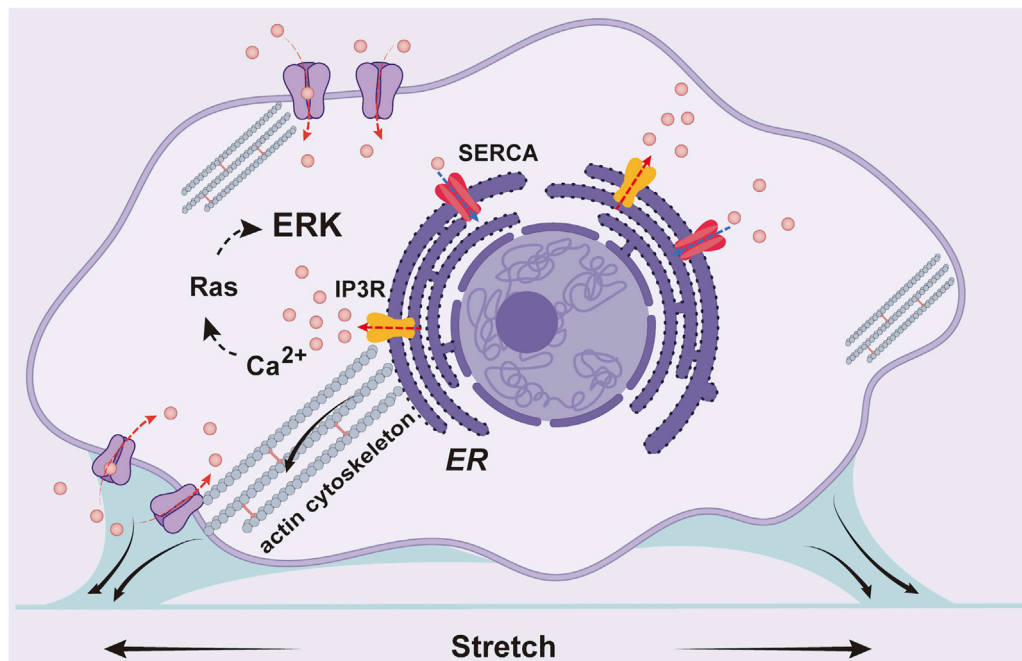


**FIGURE 7** | A schematic illustration for the mechanical activation of ERK in ASM cells. The cyclic stretch applied on the cells activates  $\text{Ca}^{2+}$  channels on the plasma and ER membranes including IP<sub>3</sub>R and SERCA pump, likely mediated by force transmission through actin cytoskeleton, and  $\text{Ca}^{2+}$  signals further trigger downstream pathway to activate ERK.

mechanical stimulations (Kim et al., 2015). By switching the culture medium to  $\text{Ca}^{2+}$ -free one before cyclic stretch, ERK activation was inhibited with a delayed response (Figures 3A,B). This suggests that  $\text{Ca}^{2+}$  channels on the plasma membrane had significant contributive role while not essential to the mechanical activation of ERK. However, by selective chemical inhibition of IP<sub>3</sub>R  $\text{Ca}^{2+}$  channel with 2-APB, or SERCA pump with Thapsigargin on ER membrane (Wang et al., 2021), the mechanical activation of ERK was almost blocked (Figures 3C,D), indicating that  $\text{Ca}^{2+}$  release from the ER store had an essential role. In contrast, there was little effect on the ERK activation by inhibition of L-type  $\text{Ca}^{2+}$  channel with nifedipine, or store-operated  $\text{Ca}^{2+}$  channel (SOC) with  $\text{LaCl}_3$  on plasma membrane (Parekh and Putney, 2005; Wang et al., 2021) (Figures 3E,F). From statistical comparison of the FRET changes (in percentage) after 0.5 h stretch and total 1 h stretch (Figure 3G), inhibition of IP<sub>3</sub>R or SERCA pump on ER membrane had the most significant impact on the mechanical activation of ERK, followed by inhibiting extracellular  $\text{Ca}^{2+}$  uptakes with reduced delayed response, while L-type  $\text{Ca}^{2+}$  channel and SOC on the plasma membrane were not actively involved into the ERK activation.

### Cyclic Stretch-Induced ERK Activation Not Dependent on PLC-IP<sub>3</sub> Signal

Since  $\text{Ca}^{2+}$  release through IP<sub>3</sub>R channel on ER membrane was essential in the stretch activation of ERK (Figure 3), we

further looked at whether inositol 1,4,5-triphosphate (IP<sub>3</sub>) production was necessary in turning on the IP<sub>3</sub>R  $\text{Ca}^{2+}$  channel. As a classic pathway, phospholipase C (PLC) is an enzyme that hydrolyzes PIP<sub>2</sub> on the plasma membrane to generate IP<sub>3</sub>, which results in opening the IP<sub>3</sub>R  $\text{Ca}^{2+}$  channel (Bartlett et al., 2020). In our experiments, inhibition of PLC activity with specific inhibitor U73122 had little effect on the cyclic stretch-induced ERK activation in comparison to the control group (Figures 4A–E). This indicates that the PLC-IP<sub>3</sub> signaling pathway was not essential in mechanical stimulation of IP<sub>3</sub>R  $\text{Ca}^{2+}$  channel for ERK activation.

### The Regulatory Role of Actin Cytoskeleton on the Mechanical Activation of ERK

Actin cytoskeleton often serves for mechanical transmission within cells (Wei et al., 2020). We hence checked the role of cytoskeleton in the mechanical activation of ERK by FRET measurements. After loss of actin cytoskeleton integrity with Cytochalasin D (Cyto D) treatment which inhibited actin filament polymerization (Supplementary Figure S5), cyclic stretch-induced ERK activation was almost completely inhibited (Figures 5A,B). Contrarily, inhibition of microtubule cytoskeleton with Nocodazole treatment did not show much effect (Figure 5C). The small GTPase Ras acts upstream of ERK through Ras-Raf-MEK-ERK signaling (Rudzka et al., 2021). The stretch-induced ERK activation was suppressed by pretreatment with Ras inhibitor Salirasib

(Figure 5D), supporting that mechanically induced  $\text{Ca}^{2+}$  signal activated ERK through Ras pathway.

## Cyclic Stretch-Induced ERK Activation Independent of Integrin $\beta 1$

Integrins are mechanosensitive molecules on plasma membrane (Sun et al., 2016; Potla et al., 2020). Integrin  $\beta 1$  (ITGB1) is a predominant subunit in forming functional heterodimers with integrin  $\alpha 1$ ,  $\alpha 2$ ,  $\alpha 11$ , and  $\alpha v$  subunits (Cai et al., 2021), so we tried to regulate the representative  $\beta 1$  to check its role in the cyclic stretch-induced activation of ERK. After knockdown of ITGB1 expression with siRNA in cells, there was no obvious impact on the cyclic stretch-induced ERK activation in comparison to the control groups (Figures 6A–C). The reduced mRNA expression of ITGB1 was confirmed by qPCR measurements (Figure 6D). Statistical quantifications confirmed no significant change in the mechanical stretch-activated ERK by ITGB1 knockdown (Figure 6E). These data indicate that integrin  $\alpha_{(x)}\beta 1$  was not the primary mechanosensor in the mechanical activation of ERK.

## DISCUSSION

The physical stretches seem critical for body health and organ homeostasis, whereas extreme stretch can be hurting as seen in sports and clinical applications (Crawford et al., 2021; Kaczka, 2021). By applying the Flexcell<sup>®</sup> tension system, we investigated cyclic stretch-induced ERK activation in ASM cells, particularly paying attention to the mechanosensitive pathway for the mechanical stimulation to biochemical signal transduction.

FRET measurements showed that ERK was efficiently activated by the mechanical stretch (Figures 2A–F). Previous studies have shown that  $\text{Ca}^{2+}$  signals in stem cells are sensitive to mechanical stimulations (Horie et al., 2016), so we checked whether  $\text{Ca}^{2+}$  channels are among the mechanosensing components for the ERK activation. Inhibition of extracellular  $\text{Ca}^{2+}$  uptakes partially reduced the mechanical activation of ERK while blocked  $\text{Ca}^{2+}$  release from the ER store had complete inhibition (Figures 3A–D). L-type  $\text{Ca}^{2+}$  channel or SOC channel on the plasma membrane was not actively engaged into the induced ERK activation (Figures 3E,F). Therefore, the mechanical stretch-induced activation of  $\text{Ca}^{2+}$  channels was essential for downstream ERK activation, which is within the mechanosensing pathway.

The  $\text{Ca}^{2+}$  channels on the ER membrane are essential for the mechanical activation of ERK (Figures 3C,D), and this observation is consistent with the previous report that  $\text{Ca}^{2+}$  signal from the ER store is induced by pulling force on the cell surface by optical laser tweezers (Kim et al., 2015). In considering that inhibition of  $\text{IP}_3\text{R}$  channel on ER blocked the ERK activation (Figure 3C), and  $\text{IP}_3$  is the ligand to turn on  $\text{IP}_3\text{R}$  channel, however, inhibition of PLC- $\text{IP}_3$  pathway had little effect (Figures 4A–E). Therefore, PLC-dependent  $\text{IP}_3$  production was not essential in the ERK activation, indicating

possibly more mechanical mechanism for ER  $\text{IP}_3\text{R}$  channel activation from cyclic stretch stimulation.

Actin cytoskeleton can pass the stretch force within the cells. Loss of actin cytoskeleton resulted in abolishing the mechanical activation of ERK, but not by loss of microtubule cytoskeleton (Figure 5), indicating that actin cytoskeleton has the crucial role on ERK activation. Possibly actin cytoskeleton passed the force to trigger the ER  $\text{Ca}^{2+}$  signals (Kim et al., 2015), which is also suggested from our data (Figures 5A–E).  $\text{Ca}^{2+}$  signals can further activate PKC to induce Ras-Raf-MEK-ERK pathway (Liao et al., 2020; Yan et al., 2020), and our data showed that inhibition of Ras truly blocked the mechanical activation of ERK (Figures 5D,E). These data indicate that actin cytoskeleton belongs to the mechanosensing component for ERK activation.

Integrins are mechanosensitive molecules and regulate focal adhesions to transmit the force inside cells (Michael et al., 2009). Integrin subunit  $\beta 1$  forms functional heterodimers with variable integrin subunits  $\alpha_{(x)}$ , so we regulated  $\beta 1$  to check its role in the stretch-induced ERK activation. Interestingly, by reduction of  $\beta 1$  expression with siRNA, there was no apparent change in the ERK activation level (Figure 6). Since cells were attached well under the siRNA transfection, the stretch force may be still transmitted efficiently to activate ERK. Previous studies reported that mechanical stretch up-regulates integrin  $\beta_{1D}$  expression to result in FAK and RhoA activations (Zhang et al., 2007), while ERK activation by mechanical stretch is independent of FAK (Hsu et al., 2010). Hence, our observation seems consistent with that. Therefore, integrin  $\alpha_{(x)}\beta 1$  did not act essentially as the primary mechanosensing component in this stretch activation of ERK in ASM cells.

## CONCLUSION

In summary, we visualized cyclic stretch-induced ERK activation by FRET biosensor in ASM cells, and provided molecular insights for the mechanosensitive pathway from mechanical stimulation to ERK biochemical activity. Data shows that  $\text{Ca}^{2+}$  channels and actin cytoskeleton are essential mechanosensing components, while integrin  $\beta 1$  is not essential in the mechanotransduction. Together with previous work, our experimental results support the following hypothesis for the mechanical activation of ERK in ASM cells (Figure 7): the cyclic stretch applied on the cells activates  $\text{Ca}^{2+}$  channels mechanically on the plasma and ER membranes, likely mediated by force transmission through actin cytoskeleton, and  $\text{Ca}^{2+}$  signals further trigger downstream signaling pathways including ERK activity in the cells.

The contributions of this work to the cyclic stretch study may be described as follows: 1) methodologically, directly visualized ERK activation by cyclic stretch in live cells at different time points with FRET biosensor, whereas previous studies were mostly done in cell lysis by using antibody detections; 2) identified that calcium channels, particularly  $\text{IP}_3\text{R}$  channel and SERCA pump on ER membrane, but not integrin  $\alpha_{(x)}\beta 1$  signals, are the primary mechanosensitive components for ERK activation, which is likely mediated *via* force transmission through actin cytoskeleton; 3) the ER  $\text{IP}_3\text{R}$  channel-dependent ERK activation does not rely on the classic upstream phospholipase C- $\text{IP}_3$  signal, indicating possibly a more mechanical

mechanism for IP<sub>3</sub>R activation by cyclic stretch. Therefore, this work provides progress in understanding this mechanical-biomechanical coupling process.

## DATA AVAILABILITY STATEMENT

The original contributions presented in the study are included in the article/**Supplementary Material**, further inquiries can be directed to the corresponding authors.

## AUTHOR CONTRIBUTIONS

MO and LD conceived the project and designed the research; XF performed the majority of experiments; XF and MO did the major data analysis and organization; YL made the nuclear ERK FRET construct; KN, YZ, and HS helped some experiments and data analysis; JG, BB, and ML provided discussion and technique support; LD provided the setup of equipment; MO, LD, and XF wrote the manuscript.

## REFERENCES

- Alexander, L. D., Alagarsamy, S., and Douglas, J. G. (2004). Cyclic Stretch-Induced cPLA2 Mediates ERK 1/2 Signaling in Rabbit Proximal Tubule Cells. *Kidney Int.* 65, 551–563. doi:10.1111/j.1523-1755.2004.00405.x
- Balestrini, A., Joseph, V., Dourado, M., Reese, R. M., Shields, S. D., Rouge, L., et al. (2021). A TRPA1 Inhibitor Suppresses Neurogenic Inflammation and Airway Contraction for Asthma Treatment. *J. Exp. Med.* 218 (4), e20201637. doi:10.1084/jem.20201637
- Bartlett, P. J., Cloete, I., Sneyd, J., and Thomas, A. P. (2020). IP<sub>3</sub>-Dependent Ca(2+) Oscillations Switch into a Dual Oscillator Mechanism in the Presence of PLC-Linked Hormones. *iScience* 23, 101062. doi:10.1016/j.isci.2020.101062
- Burgess, J. K., Lee, J. H., Ge, Q., Ramsay, E. E., Poniris, M. H., Parmentier, J., et al. (2008). Dual ERK and Phosphatidylinositol 3-kinase Pathways Control Airway Smooth Muscle Proliferation: Differences in Asthma. *J. Cel. Physiol.* 216, 673–679. doi:10.1002/jcp.21450
- Cai, C., Sun, H., Hu, L., and Fan, Z. (2021). Visualization of Integrin Molecules by Fluorescence Imaging and Techniques. *Biocell* 45, 229–257. doi:10.32604/biocell.2021.014338
- Chu, S.-Y., Chou, C.-H., Huang, H.-D., Yen, M.-H., Hong, H.-C., Chao, P.-H., et al. (2019). Mechanical Stretch Induces Hair Regeneration through the Alternative Activation of Macrophages. *Nat. Commun.* 10, 1524. doi:10.1038/s41467-019-09402-8
- Correa-Meyer, E., Pesce, L., Guerrero, C., and Sznajder, J. I. (2002). Cyclic Stretch Activates ERK1/2 via G Proteins and EGFR in Alveolar Epithelial Cells. *Am. J. Physiol. Lung Cel Mol Physiol* 282, L883–L891. doi:10.1152/ajplung.00203.2001
- Crawford, S. K., Wille, C. M., Stiffler-Joachim, M. R., Lee, K. S., Bashford, G. R., and Heiderscheit, B. C. (2021). Spatial Frequency Analysis Detects Altered Tissue Organization Following Hamstring Strain Injury at Time of Injury but Not Return to Sport. *BMC Med. Imaging* 21, 190. doi:10.1186/s12880-021-00721-1
- Dalagiorou, G., Piperi, C., Adamopoulos, C., Georgopoulou, U., Gargalionis, A. N., Spyropoulou, A., et al. (2017). Mechanosensor Polycystin-1 Potentiates Differentiation of Human Osteoblastic Cells by Upregulating Runx2 Expression via Induction of JAK2/STAT3 Signaling Axis. *Cell. Mol. Life Sci.* 74, 921–936. doi:10.1007/s00018-016-2394-8
- Dalagiorou, G., Piperi, C., Georgopoulou, U., Adamopoulos, C., Basdra, E. K., and Papavassiliou, A. G. (2013). Mechanical Stimulation of Polycystin-1 Induces Human Osteoblastic Gene Expression via Potentiation of the Calcineurin/NFAT Signaling axis. *Cel. Mol. Life Sci.* 70, 167–180. doi:10.1007/s00018-012-1164-5

## FUNDING

This work was supported financially by the National Natural Science Foundation of China (NSFC 11872129, 11532003, 1902051) and partially by the Natural Science Foundation of Jiangsu Province (BK20181416), and the Jiangsu Provincial Department of Education.

## ACKNOWLEDGMENTS

We appreciate Lei Liu, Jingjing Li, and Yan Pan at Changzhou University for experimental assistances.

## SUPPLEMENTARY MATERIAL

The Supplementary Material for this article can be found online at: <https://www.frontiersin.org/articles/10.3389/fcell.2022.847852/full#supplementary-material>

- Diem, K., Fauler, M., Fois, G., Hellmann, A., Winokur, N., Schumacher, S., et al. (2020). Mechanical Stretch Activates Piezo1 in Caveolae of Alveolar Type I Cells to Trigger ATP Release and Paracrine Stimulation of Surfactant Secretion from Alveolar Type II Cells. *FASEB J.* 34, 12785–12804. doi:10.1096/fj.202000613rrr
- Doeing, D. C., and Solway, J. (2013). Airway Smooth Muscle in the Pathophysiology and Treatment of Asthma. *J. Appl. Physiol.* (1985) 114, 834–843. doi:10.1152/japplphysiol.00950.2012
- Du, G., Li, L., Zhang, X., Liu, J., Hao, J., Zhu, J., et al. (2020). Roles of TRPV4 and Piezo Channels in Stretch-Evoked Ca(2+) Response in Chondrocytes. *Exp. Biol. Med. (Maywood)* 245, 180–189. doi:10.1177/1535370219892601
- Fang, Y., Wu, D., and Birukov, K. G. (2019). Mechanosensing and Mechanoregulation of Endothelial Cell Functions. *Compr. Physiol.* 9 (2), 873–904. doi:10.1002/cphy.c180020
- Geneen, L. J., Moore, R. A., Clarke, C., Martin, D., Colvin, L. A., and Smith, B. H. (2017). Physical Activity and Exercise for Chronic Pain in Adults: An Overview of Cochrane Reviews. *Cochrane Database Syst. Rev.* 4, CD011279. doi:10.1002/14651858.CD011279.pub3
- Hayakawa, K., Sato, N., and Obinata, T. (2001). Dynamic Reorientation of Cultured Cells and Stress Fibers under Mechanical Stress from Periodic Stretching. *Exp. Cel Res.* 268, 104–114. doi:10.1006/excr.2001.5270
- Hirata, H., Gupta, M., Vedula, S. R. K., Lim, C. T., Ladoux, B., and Sokabe, M. (2015). Actomyosin Bundles Serve as a Tension Sensor and a Platform for ERK Activation. *EMBO Rep.* 16, 250–257. doi:10.15252/embr.201439140
- Horie, S., Ansari, B., Masterson, C., Devaney, J., Scully, M., O'Toole, D., et al. (2016). Hypercapnic Acidosis Attenuates Pulmonary Epithelial Stretch-Induced Injury via Inhibition of the Canonical NF-κB Pathway. *Intensive Care Med. Exp.* 4, 8. doi:10.1186/s40635-016-0081-6
- Hsu, H.-J., Lee, C.-F., Locke, A., Vanderzyl, S. Q., and Kaunas, R. (2010). Stretch-Induced Stress Fiber Remodeling and the Activations of JNK and ERK Depend on Mechanical Strain Rate, but Not FAK. *PLoS One* 5, e12470. doi:10.1371/journal.pone.0012470
- Ingber, D. (2003). Mechanobiology and Diseases of Mechanotransduction. *Ann. Med.* 35, 564–577. doi:10.1080/07853890310016333
- Jungbauer, S., Gao, H., Spatz, J. P., and Kemkemer, R. (2008). Two Characteristic Regimes in Frequency-Dependent Dynamic Reorientation of Fibroblasts on Cyclically Stretched Substrates. *Biophysical J.* 95, 3470–3478. doi:10.1529/biophysj.107.128611
- Kaczka, D. W. (2021). Oscillatory Ventilation Redux: Alternative Perspectives on Ventilator-Induced Lung Injury in the Acute Respiratory Distress Syndrome. *Curr. Opin. Physiol.* 21, 36–43. doi:10.1016/j.cophys.2021.03.006

- Kardas, G., Daszyńska-Kardas, A., Marynowski, M., Brząkalska, O., Kuna, P., and Panek, M. (2020). Role of Platelet-Derived Growth Factor (PDGF) in Asthma as an Immunoregulatory Factor Mediating Airway Remodeling and Possible Pharmacological Target. *Front. Pharmacol.* 11, 47. doi:10.3389/fphar.2020.00047
- Kim, J., Adams, A. A., Gokina, P., Zambrano, B., Jayakumaran, J., Dobrowolski, R., et al. (2020). Mechanical Stretch Induces Myelin Protein Loss in Oligodendrocytes by Activating Erk1/2 in a Calcium-Dependent Manner. *Glia* 68, 2070–2085. doi:10.1002/glia.23827
- Kim, T. J., Joo, C., Seong, J., Vafabakhsh, R., Botvinick, E. L., Berns, M. W., et al. (2015). Distinct Mechanisms Regulating Mechanical Force-Induced Ca<sup>2+</sup> Signals at the Plasma Membrane and the ER in Human MSCs. *Elife* 4, e04876. doi:10.7554/eLife.04876
- Komatsu, N., Aoki, K., Yamada, M., Yukinaga, H., Fujita, Y., Kamioka, Y., et al. (2011). Development of an Optimized Backbone of FRET Biosensors for Kinases and GTPases. *Mol. Biol. Cell* 22, 4647–4656. doi:10.1091/mbc.e11-01-0072
- Korff, T., Aufgebauer, K., and Hecker, M. (2007). Cyclic Stretch Controls the Expression of CD40 in Endothelial Cells by Changing Their Transforming Growth Factor- $\beta$  Response. *Circulation* 116, 2288–2297. doi:10.1161/circulationaha.107.730309
- Lee, J.-H., Johnson, P. R. A., Roth, M., Hunt, N. H., and Black, J. L. (2001). ERK Activation and Mitogenesis in Human Airway Smooth Muscle Cells. *Am. J. Physiol. Lung Cell Mol Physiol* 280, L1019–L1029. doi:10.1152/ajplung.2001.280.5.L1019
- Li, Y. Y., Liu, X. S., Liu, C., Xu, Y. J., and Xiong, W. N. (2010). Role of Extracellular Signal-Regulated Kinase in Regulating Expression of Interleukin 13 in Lymphocytes from an Asthmatic Rat Model. *Chin. Med. J. (Engl)* 123, 1715–1719.
- Liang, X., Wang, Z., Gao, M., Wu, S., Zhang, J., Liu, Q., et al. (2019). Cyclic Stretch Induced Oxidative Stress by Mitochondrial and NADPH Oxidase in Retinal Pigment Epithelial Cells. *BMC Ophthalmol.* 19, 79. doi:10.1186/s12886-019-1087-0
- Liao, W.-H., Hsiao, M.-Y., Kung, Y., Liu, H.-L., Béra, J.-C., Inserra, C., et al. (2020). TRPV4 Promotes Acoustic Wave-Mediated BBB Opening via Ca(2+)/PKC-delta Pathway. *J. Adv. Res.* 26, 15–28. doi:10.1016/j.jare.2020.06.012
- Liu, B., Qu, M.-J., Qin, K.-R., Li, H., Li, Z.-K., Shen, B.-R., et al. (2008). Role of Cyclic Strain Frequency in Regulating the Alignment of Vascular Smooth Muscle Cells *In Vitro*. *Biophysical J.* 94, 1497–1507. doi:10.1529/biophysj.106.098574
- Liu, J.-T., Bao, H., Fan, Y.-J., Li, Z.-T., Yao, Q.-P., Han, Y., et al. (2021). Platelet-Derived Microvesicles Promote VSMC Dedifferentiation after Intimal Injury via Src/Lamtor1/mTORC1 Signaling. *Front. Cell Dev. Biol.* 9, 744320. doi:10.3389/fcell.2021.744320
- Liu, W., Xiong, S., Zhang, Y., Du, J., Dong, C., Yu, Z., et al. (2021). Transcriptome Profiling Reveals Important Transcription Factors and Biological Processes in Skin Regeneration Mediated by Mechanical Stretch. *Front. Genet.* 12, 757350. doi:10.3389/fgene.2021.757350
- Loperena, R., Van Beusecum, J. P., Itani, H. A., Engel, N., Laroumanie, F., Xiao, L., et al. (2018). Hypertension and Increased Endothelial Mechanical Stretch Promote Monocyte Differentiation and Activation: Roles of STAT3, Interleukin 6 and Hydrogen Peroxide. *Cardiovasc. Res.* 114, 1547–1563. doi:10.1093/cvr/cvy112
- Luo, L., Li, E., Zhao, S., Wang, J., Zhu, Z., Liu, Y., et al. (2018). Gasoline Exhaust Damages Spermatogenesis through Downregulating  $\alpha$ 6-Integrin and  $\beta$ 1-Integrin in the Rat Model. *Andrologia* 50, e13045. doi:10.1111/and.13045
- Mammoto, T., Mammoto, A., and Ingber, D. E. (2013). Mechanobiology and Developmental Control. *Annu. Rev. Cell Dev. Biol.* 29, 27–61. doi:10.1146/annurev-cellbio-101512-122340
- Michael, K. E., Dumbauld, D. W., Burns, K. L., Hanks, S. K., and García, A. J. (2009). Focal Adhesion Kinase Modulates Cell Adhesion Strengthening via Integrin Activation. *Mol. Biol. Cell* 20, 2508–2519. doi:10.1091/mbc.e08-01-0076
- Ouyang, M., Wan, R., Qin, Q., Peng, Q., Wang, P., Wu, J., et al. (2019). Sensitive FRET Biosensor Reveals Fyn Kinase Regulation by Submembrane Localization. *ACS Sens.* 4, 76–86. doi:10.1021/acssensors.8b00896
- Parekh, A. B., and Putney, J. W., Jr. (2005). Store-Operated Calcium Channels. *Physiol. Rev.* 85, 757–810. doi:10.1152/physrev.00057.2003
- Ponsioen, B., Post, J. B., Buissant des Amorie, J. R., Laskaris, D., van Ineveld, R. L., Kersten, S., et al. (2021). Quantifying Single-Cell ERK Dynamics in Colorectal Cancer Organoids Reveals EGFR as an Amplifier of Oncogenic MAPK Pathway Signalling. *Nat. Cell Biol* 23, 377–390. doi:10.1038/s41556-021-00654-5
- Potla, R., Hirano-Kobayashi, M., Wu, H., Chen, H., Mammoto, A., Matthews, B. D., et al. (2020). Molecular Mapping of Transmembrane Mechanotransduction through the  $\beta$ 1 Integrin-CD98hc-TRPV4 Axis. *J. Cell Sci* 133. doi:10.1242/jcs.248823
- Qi, Y.-X., Yao, Q.-P., Huang, K., Shi, Q., Zhang, P., Wang, G.-L., et al. (2016). Nuclear Envelope Proteins Modulate Proliferation of Vascular Smooth Muscle Cells during Cyclic Stretch Application. *Proc. Natl. Acad. Sci. U.S.A.* 113, 5293–5298. doi:10.1073/pnas.1604569113
- Qin, Q., Laub, S., Shi, Y., Ouyang, M., Peng, Q., Zhang, J., et al. (2019). Fluocell for Ratiometric and High-Throughput Live-Cell Image Visualization and Quantitation. *Front. Phys.* 7, 154. doi:10.3389/fphy.2019.00154
- Ren, D., Song, J., Liu, R., Zeng, X., Yan, X., Zhang, Q., et al. (2021). Molecular and Biomechanical Adaptations to Mechanical Stretch in Cultured Myotubes. *Front. Physiol.* 12, 689492. doi:10.3389/fphys.2021.689492
- Rudzka, D. A., Mason, S., Neilson, M., McGarry, L., Kalna, G., Hedley, A., et al. (2021). Selection of Established Tumour Cells through Narrow Diameter Micropores Enriches for Elevated Ras/Raf/MEK/ERK MAPK Signalling and Enhanced Tumour Growth. *Small GTPases* 12, 294–310. doi:10.1080/21541248.2020.1780108
- Sadoshima, J., and Izumo, S. (1993). Mechanical Stretch Rapidly Activates Multiple Signal Transduction Pathways in Cardiac Myocytes: Potential Involvement of an Autocrine/Paracrine Mechanism. *EMBO J.* 12, 1681–1692. doi:10.1002/j.1460-2075.1993.tb05813.x
- Schmidt, J. B., Chen, K., and Tranquillo, R. T. (2016). Effects of Intermittent and Incremental Cyclic Stretch on ERK Signaling and Collagen Production in Engineered Tissue. *Cell. Mol. Bioeng.* 9, 55–64. doi:10.1007/s12195-015-0415-6
- Slutsky, A. S., and Ranieri, V. M. (2014). Ventilator-Induced Lung Injury. *N. Engl. J. Med.* 370, 980. doi:10.1056/NEJMc1400293
- Sun, Z., Guo, S. S., and Fässler, R. (2016). Integrin-Mediated Mechanotransduction. *J. Cell Biol.* 215, 445–456. doi:10.1083/jcb.201609037
- Swaminathan, V., and Glierich, M. (2021). Decoding Mechanical Cues by Molecular Mechanotransduction. *Curr. Opin. Cell Biol.* 72, 72–80. doi:10.1016/j.cob.2021.05.006
- Takahara, N., Ito, S., Furuya, K., Naruse, K., Aso, H., Kondo, M., et al. (2014). Real-Time Imaging of ATP Release Induced by Mechanical Stretch in Human Airway Smooth Muscle Cells. *Am. J. Respir. Cell Mol Biol* 51, 772–782. doi:10.1165/rcmb.2014-0008oc
- Wang, J. H.-C., Goldschmidt-Clermont, P., Wille, J., and Yin, F. C.-P. (2001). Specificity of Endothelial Cell Reorientation in Response to Cyclic Mechanical Stretching. *J. Biomech.* 34, 1563–1572. doi:10.1016/s0021-9290(01)00150-6
- Wang, L., Bao, H., Wang, K.-X., Zhang, P., Yao, Q.-P., Chen, X.-H., et al. (2017). Secreted miR-27a Induced by Cyclic Stretch Modulates the Proliferation of Endothelial Cells in Hypertension via GRK6. *Sci. Rep.* 7, 41058. doi:10.1038/srep41058
- Wang, M., Sun, Y., Li, L., Wu, P., Dkw, O., and Shi, H. (2021). Calcium Channels: Noteworthy Regulators and Therapeutic Targets in Dermatological Diseases. *Front. Pharmacol.* 12, 702264. doi:10.3389/fphar.2021.702264
- Wang, Y., Lu, Y., Luo, M., Shi, X., Pan, Y., Zeng, H., et al. (2016). Evaluation of Pharmacological Relaxation Effect of the Natural Product Naringin on *In Vitro* Cultured Airway Smooth Muscle Cells and *In Vivo* Ovalbumin-Induced Asthma Balb/c Mice. *Biomed. Rep.* 5, 715–722. doi:10.3892/br.2016.797
- Wei, F., Xu, X., Zhang, C., Liao, Y., Ji, B., and Wang, N. (2020). Stress Fiber Anisotropy Contributes to Force-Mode Dependent Chromatin Stretching and Gene Upregulation in Living Cells. *Nat. Commun.* 11, 4902. doi:10.1038/s41467-020-18584-5
- Yan, A., Song, L., Zhang, Y., Wang, X., and Liu, Z. (2020). Systemic Inflammation Increases the Susceptibility to Levodopa-Induced Dyskinesia in 6-OHDA Lesioned Rats by Targeting the NR2B-Medicated PKC/MEK/ERK Pathway. *Front. Aging Neurosci.* 12, 625166. doi:10.3389/fnagi.2020.625166
- Yao, H., Wang, L., Guo, J., Liu, W., Li, J., Wang, Y., et al. (2020). Genetically Encoded FRET Biosensor Detects the Enzymatic Activity of Prostate-

- Specific Antigen. *Mol. Cell Biomech.* 17, 101–111. doi:10.32604/mcb.2020.09595
- Zhang, S. J., Truskey, G. A., and Kraus, W. E. (2007). Effect of Cyclic Stretch on  $\beta$ 1D-Integrin Expression and Activation of FAK and RhoA. *Am. J. Physiology-Cell Physiol.* 292, C2057–C2069. doi:10.1152/ajpcell.00493.2006
- Zuyderduyn, S., Sukkar, M. B., Fust, A., Dhaliwal, S., and Burgess, J. K. (2008). Treating Asthma Means Treating Airway Smooth Muscle Cells. *Eur. Respir. J.* 32, 265–274. doi:10.1183/09031936.00051407

**Conflict of Interest:** The authors declare that the research was conducted in the absence of any commercial or financial relationships that could be construed as a potential conflict of interest.

**Publisher's Note:** All claims expressed in this article are solely those of the authors and do not necessarily represent those of their affiliated organizations, or those of the publisher, the editors, and the reviewers. Any product that may be evaluated in this article, or claim that may be made by its manufacturer, is not guaranteed or endorsed by the publisher.

Copyright © 2022 Fang, Ni, Guo, Li, Zhou, Sheng, Bu, Luo, Ouyang and Deng. This is an open-access article distributed under the terms of the Creative Commons Attribution License (CC BY). The use, distribution or reproduction in other forums is permitted, provided the original author(s) and the copyright owner(s) are credited and that the original publication in this journal is cited, in accordance with accepted academic practice. No use, distribution or reproduction is permitted which does not comply with these terms.